18

Machining and Machinability of Aluminum Alloys

V. Songmene, R. Khettabi, I. Zaghbani, J. Kouam, and A. Djebara
École de technologie supérieure (ÉTS), Department of Mechanical Engineering,
1100 Notre-Dame Street West, Montreal Quebec H3C 1K3
Canada

1. Introduction

The use of materials with low specific weight is an effective way of reducing the weight of structures. Aluminum alloys are among the most commonly used lightweight metallic materials as they offer a number of different interesting mechanical and thermal properties. In addition, they are relatively easy to shape metals, especially in material removal processes, such as machining. In fact, aluminum alloys as a class are considered as the family of materials offering the highest levels of machinability, as compared to other families of lightweight metals such as titanium and magnesium alloys. This machinability quantifies the machining performance, and may be defined for a specific application by various criteria, such as tool life, surface finish, chip evacuation, material removal rate and machine-tool power. It has been shown that chemical composition, structural defects and alloying elements significantly influence machinability [W Konig et al., 1983]. Thus, with similar chemical compositions, the machinability of alloys can be improved by different treatments. Heat treatments, which increase hardness, will reduce the built-up edge (BUE) tendency during machining [M. Tash et al., 2006]. In the case of dry machining, the major problems encountered are the BUE at low cutting speeds and sticking at high cutting speeds, hence the need for special tool geometries [P. Roy et al., 2008]. It has been shown that high levels of Magnesium (Mg) increase the cutting forces at the same level of hardness [M. Tash et al., 2006], while a low percentage of Copper (Cu) in aluminum alloy 319 decreases the cutting force. Similarly, it has been found that heat treatment of 6061, especially aging, influences the forces only at low cutting speeds, while at high speeds, the influence is negligible because of the low temperature rise seen in the cutting zone [Demir H et al., 2008]. Cutting force is just one among several parameters to be considered for a full assessment of the machinability of metallic alloys, with the others being the tool life, the surface finish, the cutting energy and the chip formation mode.

Aluminum alloys are classified under two classes: cast alloys and wrought alloys. Furthermore, they can be classified according to the specification of the alloying elements involved, such as strain-hardenable alloys and heat-treatable alloys. Most wrought aluminum alloys have excellent machinability. While cast alloys containing copper, magnesium or zinc as the main alloying elements can cause some machining difficulties, the use of small tool rake angles can however improve machinability. Alloys having silicon as the main alloying element involve larger tool rake angles, lower speeds and feeds, making them more cost-effective to machine. Aluminum alloys, which are not sensitive to heat treatments, can be hardened by cold work that can improve their machinability when sharp tools are used. Following (ASM Handbook, Volume 16) the machinability of different aluminum alloys has been treated in general manner with a classification (A, B, C, D and E) according to the alloy state. Traditionally, the machinability of materials involve tool life, cutting forces, productivity or chip form, with less attention paid to particle emission. In this work, the authors address the machinability of aluminum alloys from several points of view, including cutting forces, chip forms and segmentation, and metallic particle emission. The following section addresses machinability, while section 3 focuses on metallic particle emission during the machining of aluminum and the effect of materials, cutting conditions and lubrication mode.

2. Machinability of aluminum alloys

2.1 Cutting force during machining of aluminum alloys

While the cutting forces during the machining of aluminum alloys are relatively low, they can nevertheless provide a good indicator for a comparison of different alloys under the same machining conditions (Zaghbani and Songmene, 2009). A typical cutting force signal acting on the cutter in the axial direction (thrust force Fz) during drilling is presented in Figure 1. Portion a-b of the graph (Fig. 1a) corresponds to the drill point engagement into the workpiece while the portion b-c corresponds to the real cutting. Portion b-c is usually employed to estimate the cutting force or the energy required to shape metals. Using an enlarged graph (Fig. 1b), it is possible to identify the action of each flute of the cutter during the cutting process.

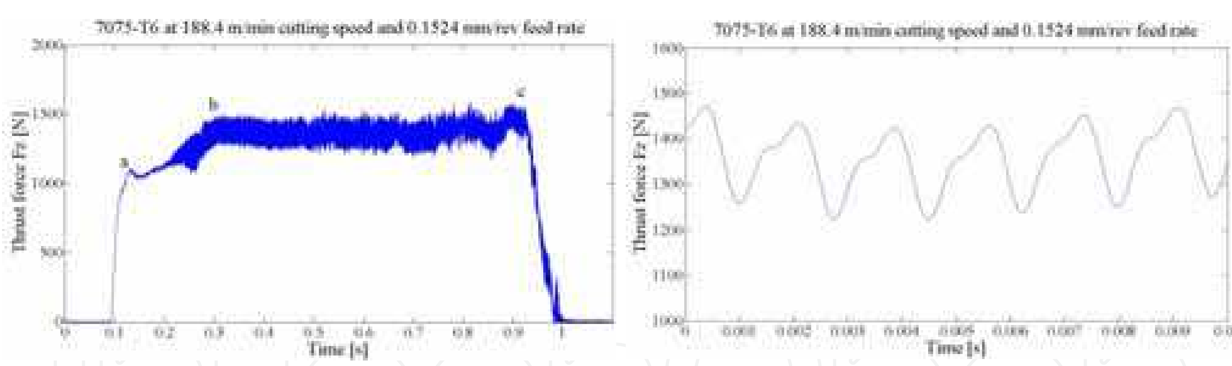

(a) (b)

Fig. 1. Typical instantaneous cutting forces during drilling of 7075-T6 aluminum alloys

The average thrust force (portion b-c of Fig. 1a) for different cutting speeds when drilling four different aluminum alloys (6061-T6, 7075-T6, A356-T0, A319-T0) is presented in Figure 2 (Kouam et al, 2010). It can be seen that only the 7075-T6 is sensitive to variations of the cutting speed, and exhibits a decrease in the average thrust force, which is probably due to the softening effect observed at relatively high speeds. The three other alloys exhibit a low sensitivity to variations of cutting speed.

The cutting forces are more sensitive to the variations of the feed. In fact, the feed determines the chip thickness, which is the major factor governing the cutting forces. Different drilling tests were performed using a High Speed Steel drill with a 10 mm diameter and a point angle of 118° in order to determine the effect of feed and alloys on cutting forces. The results obtained are presented in Figure 3. As expected, the thrust force increases with the feed rate at different cutting speeds for all tested materials. These results (Fig. 3) confirm the previous works of different authors (M.C. Shaw, 1989; E. J A. Armarego, 1984; Subramnian et al., 1977 and Balout et al., 2002). The thrust force (F_z) increases as the feed rate increases for the cast and wrought materials.

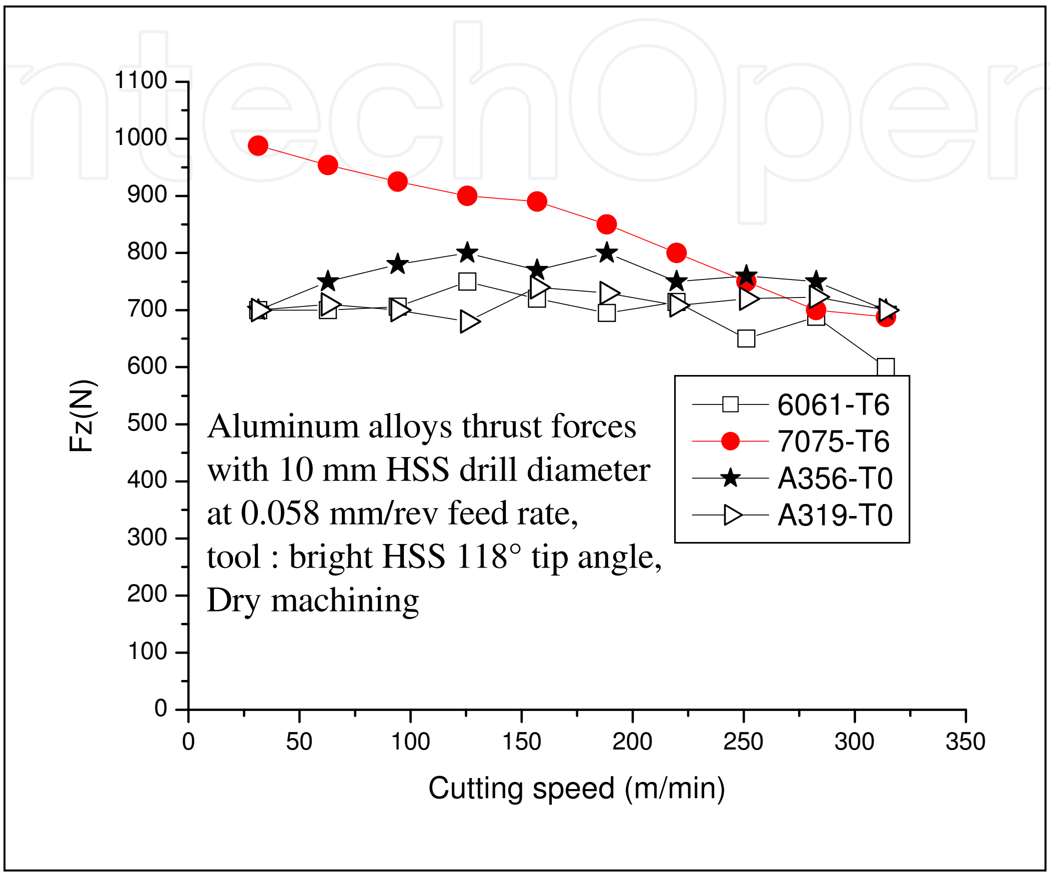

Fig. 2. Thrust force Fz at different cutting speeds for 6061-T6 material, 7075-T6 material, A356-T0 material and A319-T0 material

2.2 Chip formation and chip segmentation

The chip shape and microstructure constitute a good indicator of the deformation having occurred during the machining process. The chip formation mode depends on the workpiece material, the tool geometry and the cutting conditions. A small and segmented chip is preferable when cutting metals. Several research works have analyzed chip formation in order to identify the optimal conditions for improving machining and machinability. Xie et al. (1996) developed a coefficient identifying chip segmentation, called the flow localization parameter β. Several tests were carried out in the laboratory in order to characterize the chip shape during the machining of aluminum alloys. Figure 4 presents the chip morphology obtained from scanning electronic microscopy (SEM) as a function of cutting speed and alloys when drilling different aluminum alloys at a feed rate of 0.15 mm/rev. It can be observed that even brittle materials, such as A356-T0 and A319-T0, can produce continuous and long chips at low cutting speeds. Similarly, more ductile materials, such as 6061-T6 and 7075-T6, can also produce discontinuous chips (in this case, at moderate speeds).

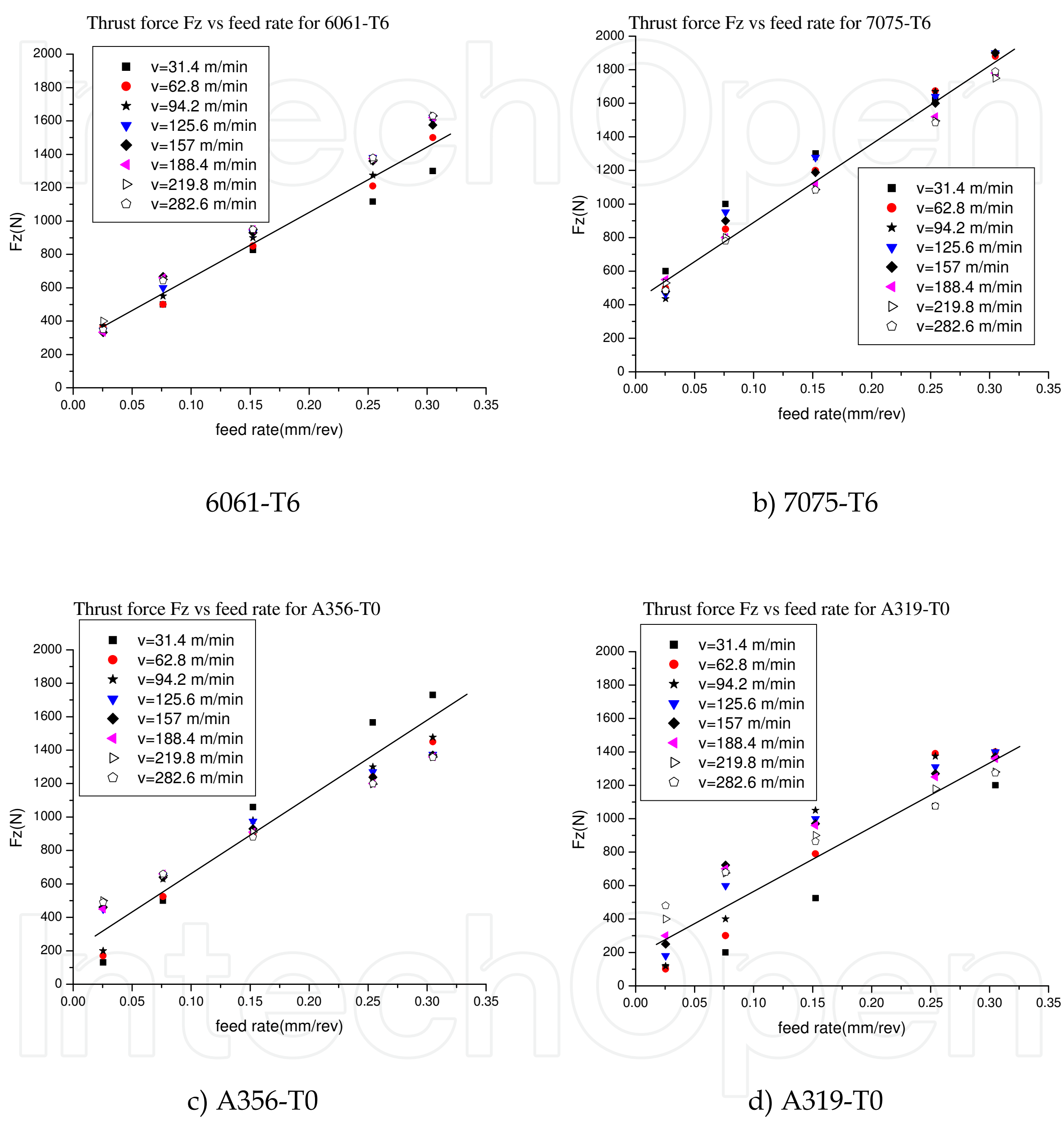

Fig. 3. Thrust force Fz at different feed rates; a- 6061-T6 material, b- 7075-T6 material, c- A356-T0 material and d- A319-T0 material.

Materials	Chip form at 31.4 m/min	Chip form at 94.2 m/min	Chip form at 188.4 m/min
6061-T6	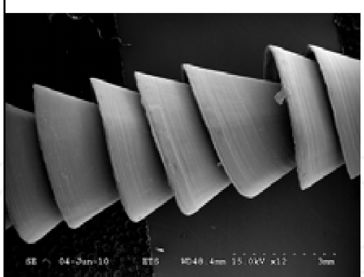	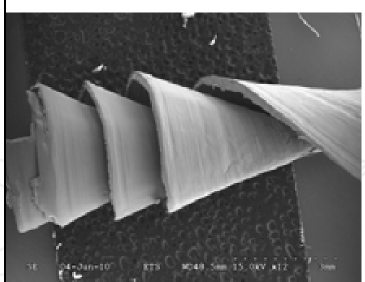	
7075-T6	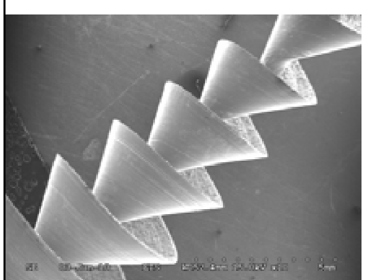	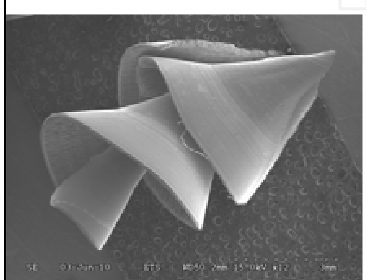	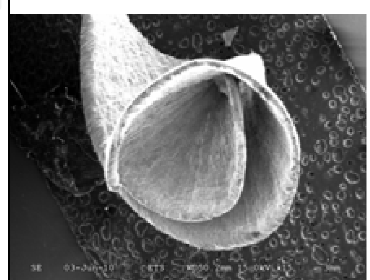
A356-T0	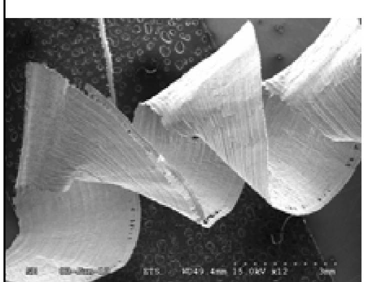	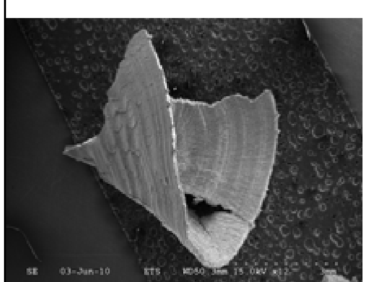	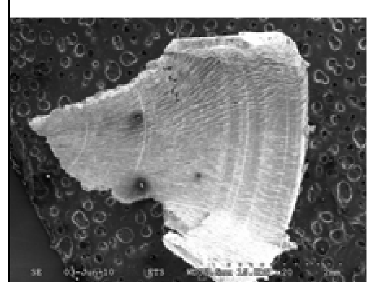
A319-T0	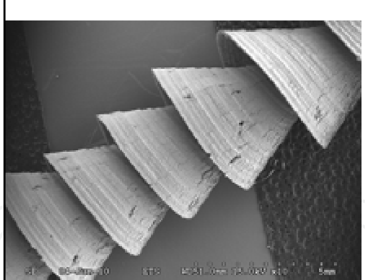	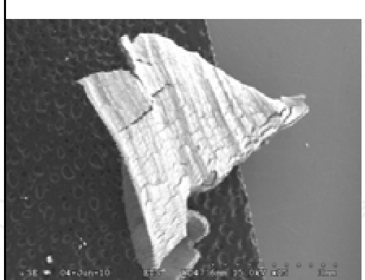	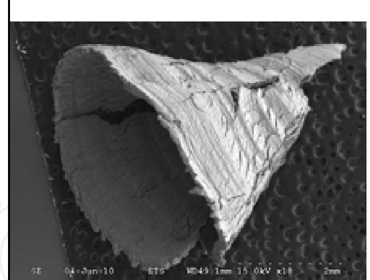

Fig. 4. SEM images of chip obtained during the drilling of aluminum alloys at 0.15 mm/rev feed rate and at different cutting speeds

Figure 5 presents different chip forms and lengths (small, middle and long chip), and is representative for the others materials. In this graph (Fig. 5), the limit zone between continuous and discontinuous chips is delimited. Such limits have made it possible to obtain experimentally Figure 6 delimitating continuous chip form zone to discontinuous chip form zone for each material tested. Determining these limits can help in selecting cutting conditions that will lead to the desired discontinuous chip. The production of discontinuous chips is recommended, especially for automated production, where easy-to-manage chip will not stop production.

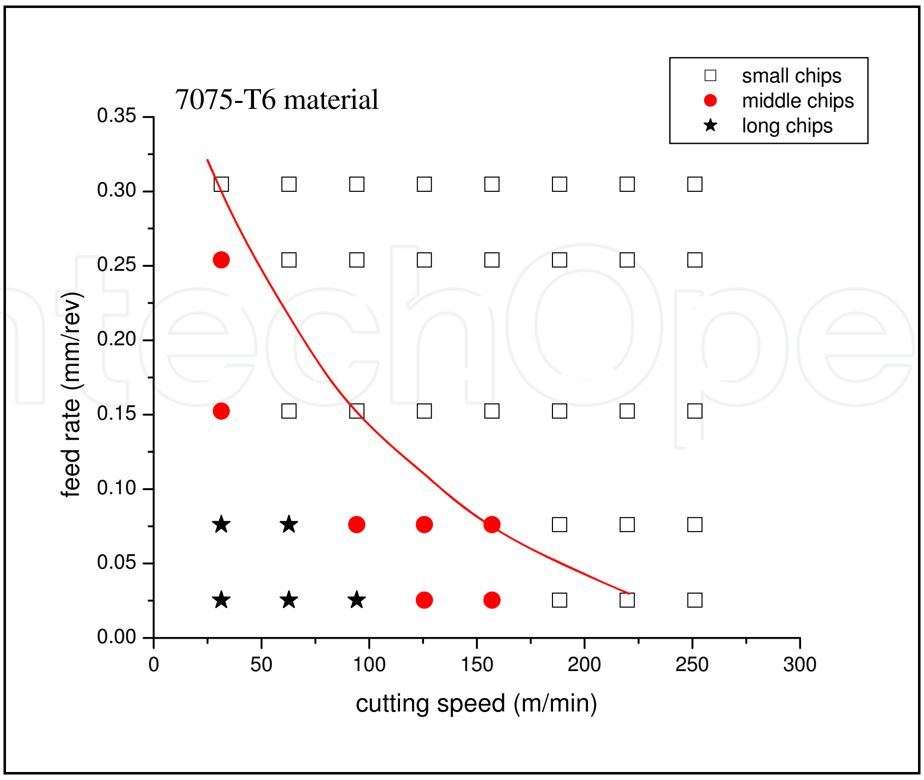

Fig. 5. Experimental chip form map for 7075-T6

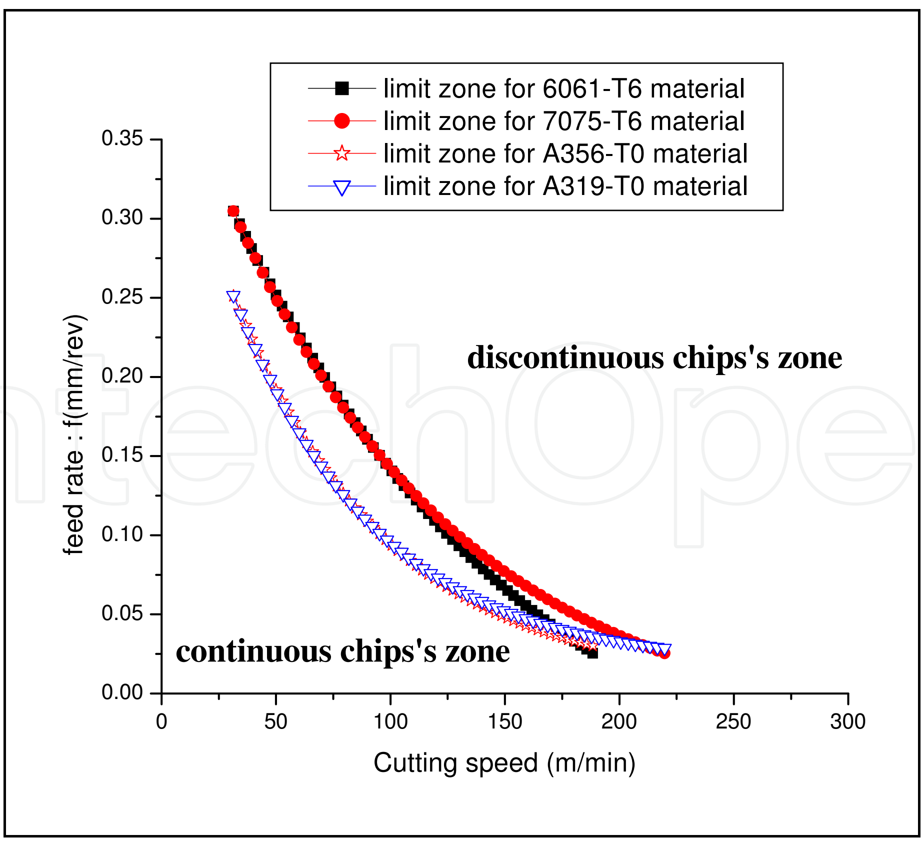

Fig. 6. Experimental chip form transition limits of different materials

It is observed in Figure 6 that at low cutting speeds, the chip is generally continuous for different materials. For 6061-T6 and 7075-T6 materials, the chip length decreases as the cutting speed increases, and it is the same for A319-T0 and A356-T0. This decrease in the length of the chip depends not only on the cutting speed, but also on the feed rate. Figure 6 suggests that the chip length depends not only on the material properties (ductility and brittleness for example) but also on the cutting conditions. Equation (1) can allow the prediction of the chip form, depending on the cutting parameters and the material used. Chip breakability is one of the major issues faced in machining aluminum alloys; in fact, long chips can cause damage to the machined surface, to the cutter and to the machine evacuation system. Chip segmentation is one of the practical tools used to compare the chip breakability of different alloys. From Figure 6, the general trend equation delimiting different chip form zones for the tested aluminum alloys can be expressed as follows:

$$f = f_0 + Ae^{-(\frac{v}{B})} \tag{1}$$

where f is the feed rate, v is the cutting speed, A and B are constants, depending on the workpiece material used. The constants of equation (1) are given as follows in Table 1:

Material	f_0(mm/rev)	A	B
6061-T6	0.00021	0.5	130.62
7075-T6	0.00033	0.45	100.48
A356-T0	0.01	0.4	65.84
A319-T0	0.02	0.4	62.80

Table 1. Constant values for different materials used in the equation (1)

The chip segmentation is schematized in Figure 8 for an orthogonal cutting process. Xie et al. (1996) found that there are some critical values of the product of the cutting speed and feed rate for which chip segmentation begins. The segmentation can also be defined by the segmentation band density. According to the formulation of Becze and Elbestawi (2002), the chip segmentation density η_s can be also estimated by the following equation:

$$\eta_S^{-1} = (A + B\exp(CV)) * \left(1 + D\left(\frac{f - f_0}{f_0}\right)\right) \tag{2}$$

where f is the feed rate, V is the cutting speed, and A, B, and C are empirical constants. Khettabi et al. (2009) developed a simple method for determining the chip segmentation density using the distance (l) corresponding to 10 segmentation bands (Eq. 3).

$$\eta_s = \frac{1}{l_b} = \frac{10}{l} \tag{3}$$

where l_b is the band width (see Fig. 7).

The chip compression ratio, the chip thickness and the tendency for segmentation during machining of 6061-T6 are presented in Table 2. The gray cells represent a continuous chip formation zone, while the white cells represent conditions at which the formation of segmented chip occurred. The chip compression ratio C_h can be calculated using Eq. 4 or estimated using Eq. 5:

$$C_h = \frac{\sin\phi}{\cos(\phi - \alpha)} \tag{4}$$

where α is the tool rake angle and ϕ is the shear angle,

$$C_h = \frac{h}{h_c} \tag{5}$$

where h is the undeformed chip thickness and h_C is the chip thickness (Fig. 8).
For the cutting of aluminum alloy 6061-T6 with a -7 rake angle, the segmentation is observable at speeds starting at 200 m/min, while for the null rake angle, observable chip segmentation starts at about 250 m/min, and for a rake angle of +7°, there is no noticeable segmentation. In the absence of a noticeable chip segmentation, the chip is continuous, while the chip is partially or completely segmented when segments are visible.

Rake angle (°)	100 m/min	150 m/min	200 m/min	250 m/min	300 m/min
-7	0.1876	0.1925	0.2081	0.2199	0.2320
0	0.2147	0.2027	0.2299	0.2330	0.2387
+7	0.2587	0.2744	0.2593	0.2806	0.2894

← Thick chip /Thin chip →

Table 2. Chip ratio (6061-T6 Aluminum)

In Table 2, the chip compression ratio is geometrically measured for the aluminum alloy 6061-T6. When the cutting speed increases, so does the chip compression ratio, and the chip becomes thin and brittle. It has been observed that when the chip becomes brittle, dust emission decreases significantly (Balout et al., 2007; Khettabi et al., 2008).
While aluminum alloys are considered easy to machine, they can generate harmful metallic particles during the machining process. There is a correlation between chip morphology, cutting parameters, machinability and dust emission. Segmented chips produce less dust, a good finish and allow better machinability than continuous chips, while an increase in the segmentation density increases dust emissions. The following section will focus on the metallic particle generation during the machining of aluminum alloys.

3. Metallic particle emission

3.1 Dust emission problem

In addition of chips, the shaping of metallic alloys, including the machining of aluminum alloys, produce metallic particles of different sizes that can be harmful to the machine tool operator. Diseases caused by exposure to dust range from simple respiratory irritation to bronchitis, asthma and cancer. Consequently, the regulatory health and safety agencies overseeing machining are requiring that more and more manufacturers reduce dust generated from manufacturing processes. A risk prevention and control committee of the World Health Organization working group held in Switzerland in 1999 (EHO, 1999) called for research into dust production process parameters, which should help assess the reliability and costs of changing systems in order to improve dust control. The United States' Environmental Protection Agency (EPA) has found that even low concentrations of certain metals can cause acute pulmonary effects.

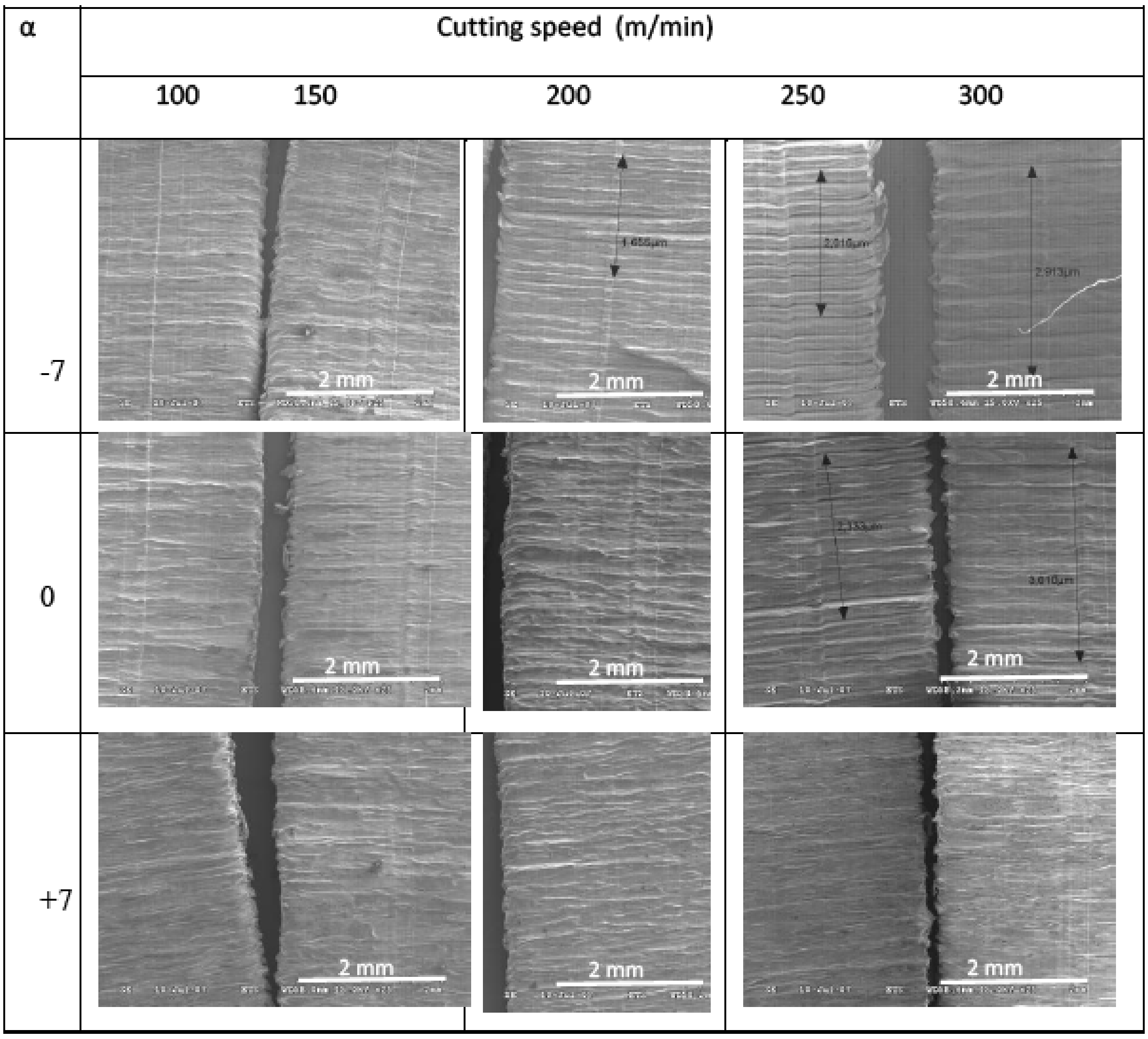

Fig. 7. Aluminum 6061-T6 chip segmentation as a function of cutting speed and tool rake angle when turning 6061-T6

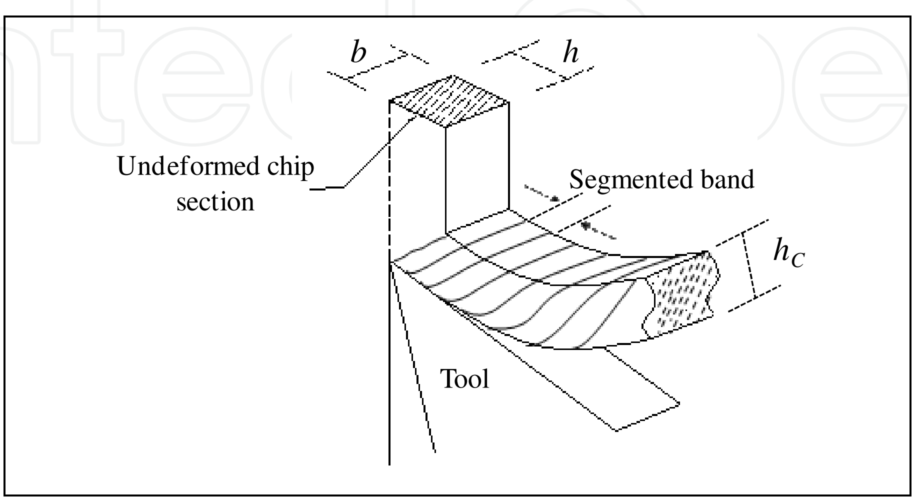

Fig. 8. Orthogonal cutting (uncut chip cross-section)

In situations where the main polluters are gases, air quality control in the industrial environment is usually carried out in free air by sampling particulate matter smaller than 2.5µm (PM 2.5) or by gas receptors. An evaluation of process emissivity must be done using high sensitivity methods. While carrying out measurements in free air (far from the cutting zone) is the usual method for air quality control, it is however not appropriate for determining the emissivity of operations and of materials. Free air measurement involves large sampling volumes, and thus considerably increases the testing time and reduces dust concentration. To identify the emission capacity of each operation in the laboratory, the system must be isolated in order to ensure that the measurements involve only the dust produced by the operation under study. For different cutting processes (Fig. 9) several sampling devices, such as laser photometers (DustTrack), APS (Aerodynamic Particle Sizer Spectrometer), MOUDI (Micro-Orifice, Uniform-Deposit Impactor), ELPI or SMPS (Scanning Mobility Particle Sizer), can be used to measure the particles produced. The measurement device could be connected to the dust recovery enclosure by a suction pipe, and a computer equipped with a data acquisition and analysis system is also connected to the measuring device. For the SMPS system, it can be possible to connect the Nanometer Aerosol Sampler (NAS) at the exit of the DMA of the SMPS in order to collect particles with specially prepared substrates allowing for microscopy analysis of generated particles. For the ELPI or the MOUDI systems, particles can be collected directly on the substrate. Figure 10 shows experimental evidence of fine and ultrafine particles generated during machining carried out in the laboratory. The AFM can show the particles in 3D (Fig. 10a) while with the SEM, it is only in 2D (Fig. 10b).

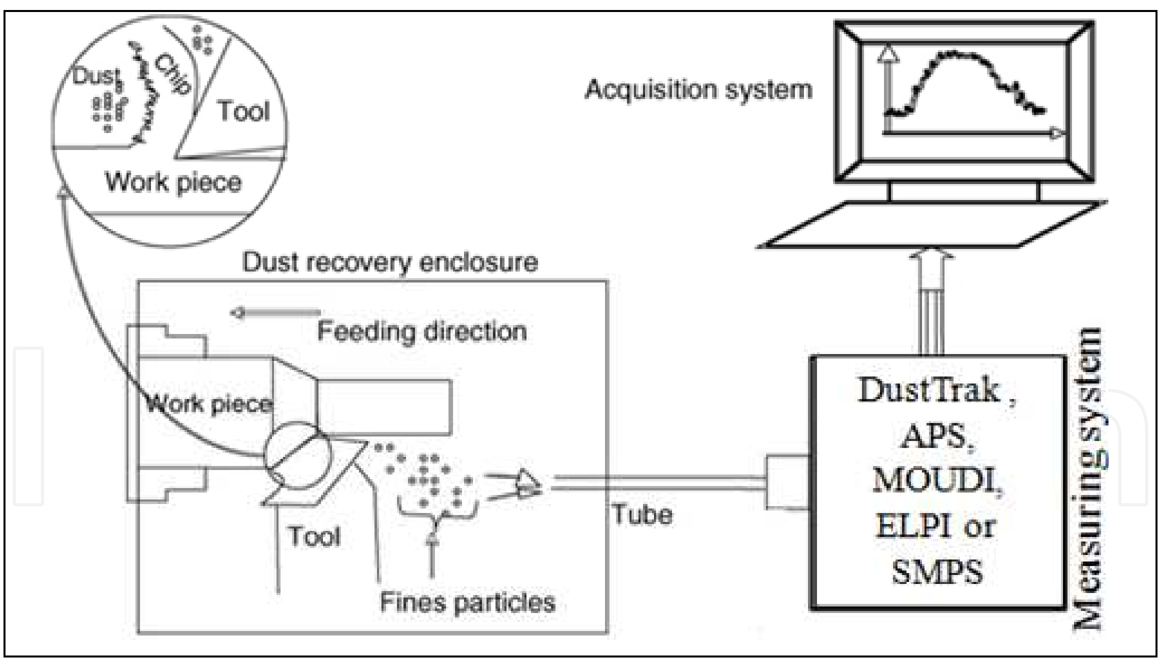

Fig. 9. Experimental set-up used for metallic particle emission test

3.2 Effects of cutting conditions and alloys

Arumugan et al. (2002) studied dust mass concentration during machining and found that the cutting speed is the most influential factor among all cutting parameters (the others being feed and depth of cut). The concentration decreased as the speed was increased in a

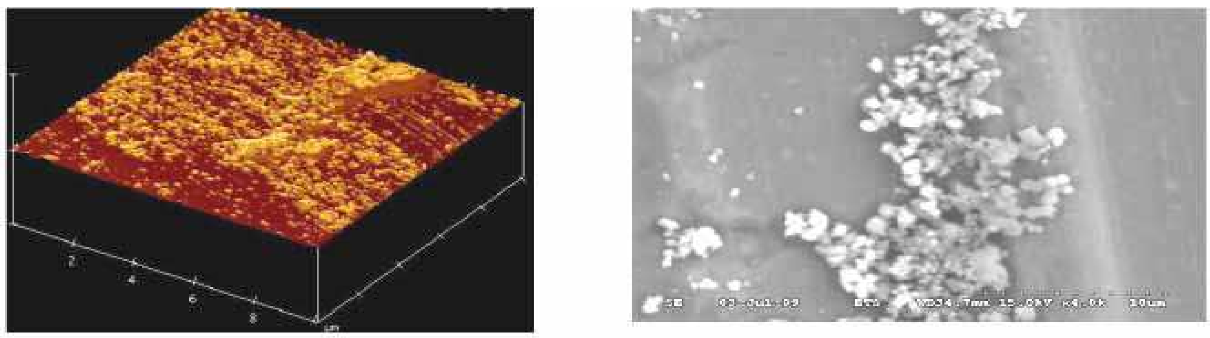

a) b)

Fig. 10. Particle shape visualization by a) AFM in 3D and b) SEM

specific feed zone. Songmene et al. (2007, 2008) found two different zones (I and III) corresponding to low and high cutting ranges, respectively, in which the dust emission is low. Between the two zones was the zone II in which the dust emission increases with the cutting speed and reached a maximum. Machining in zone I (low cutting speeds) is not recommended because productivity would be reduced. In zone III (high cutting speeds), which is the recommended zone, the dust emission decreases while the productivity and the part quality are improved. Therefore, high speed machining is not only good for improving productivity and lowering the cutting forces and energy consumption, but also for protecting the environment and worker health.

Khettabi et al. (2009) found the same link between dust emission and cutting speed during the turning of aluminum alloys and steels. The result was also confirmed during the dry machining of aluminum alloys and steel materials (Figure 11).

The concentration of particle emissions was found to be higher for wet machining than for dry machining for sub-micron size particles (Zaghbani et al., 2009b). For this size range, the particle mass concentration is 5 to 30 times greater for wet than for dry milling. However, for micronic particles, the mass concentration of particles generated in wet milling is lower than the particle mass concentration in dry milling. Consequently, the cutting fluid allows the generation of more sub-micron wet and dry particles (Fig. 12).

3.3 Understanding and modeling particle emissions

The formation of fine and ultrafine particles during machining is attributable to different phenomena, such as: macroscopic and microscopic friction, plastic deformation and chip formation mode. The friction of the chip micro-segments between themselves produces micrometric and nanometric sized particles. Similarly, the friction at the tool rake face with the chip also produces particles. Figure 13 can give an illustration of the dust emission mechanisms by friction of the chip on the tool rake face.

Particle formation by friction proceeds through two main steps, depending on the workpiece material: step 1 occurs during the material separation while step 2 takes place when the chip slides on the tool rake face. In the case of brittle materials, the chip is formed by brittle fracture, with the chip contact length being very small. In this situation, the contact between the tool material and the irregular chip surface can break up particles from the internal chip surface. If the workpiece material is ductile, the chip will be formed by micro-segments that undergo a local work hardening due to the action of some asperities of the tool rake face. Then, the hardened small part is separated by a local brittle fracture. This

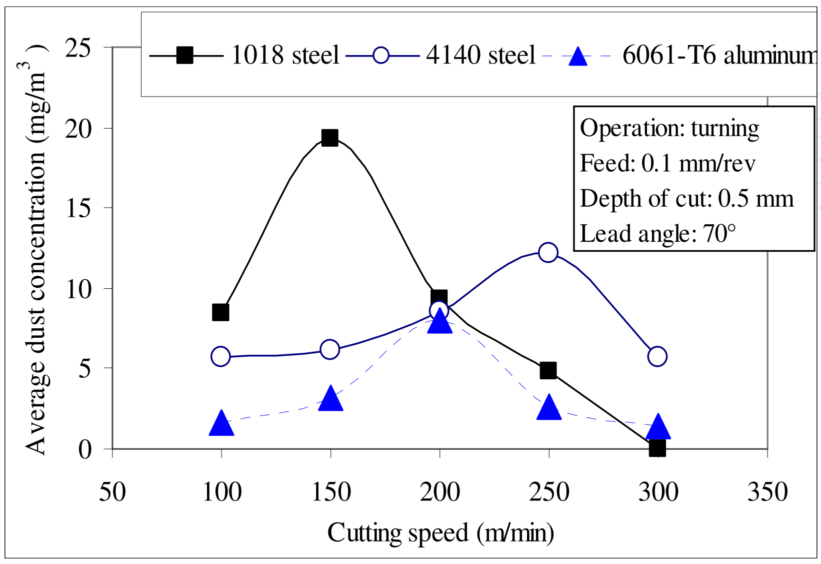

a)

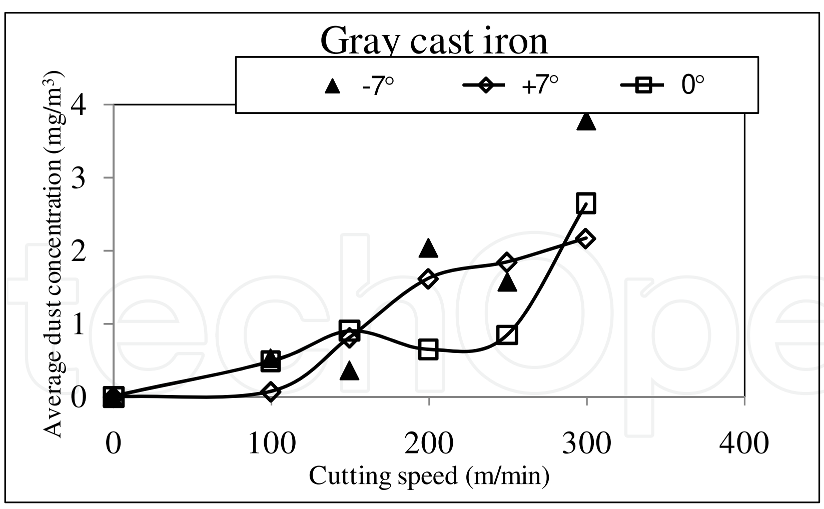

b)

Fig. 11. Average dust concentration (PM2.5) as a function of cutting speed when turning a) steels and 6061-T6 aluminum and b) gray cast iron.

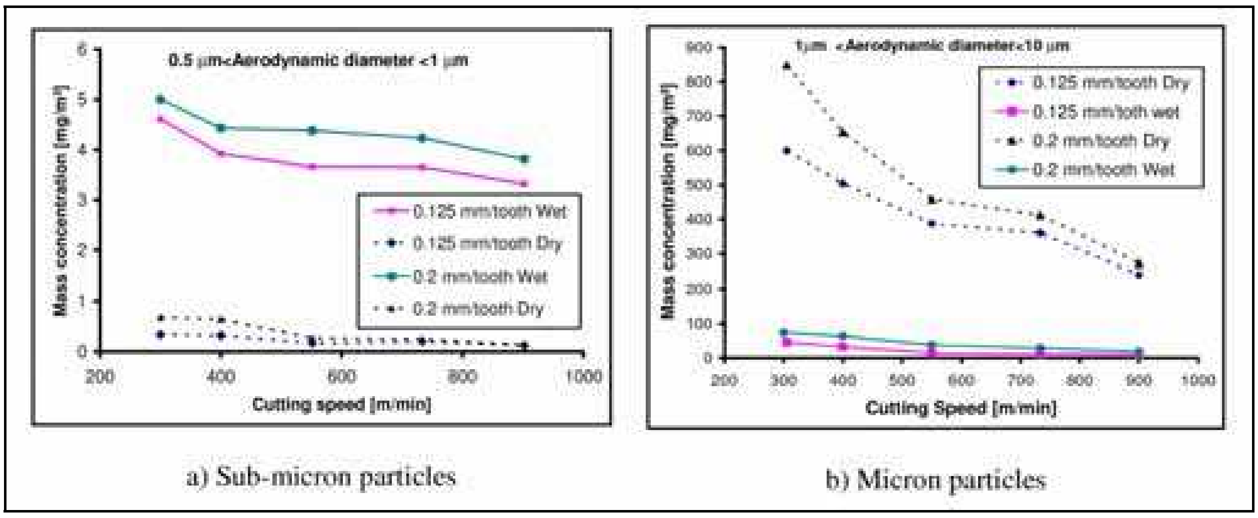

Fig. 12. Influence of the cutting speed on mass concentration for different particle sizes

mechanism describes how friction or micro-friction can produce small particles during machining. The size of the particles separated depends on the tool rake face roughness, the cutting conditions, and the workpiece material.

The dust generation mechanism is not caused purely by the mechanical effect, as the temperature of the chip formation zone also plays a big role in this mechanism. The temperature involved in the cutting process alters the mechanical properties of the material, and modifies the chip formation mode and the particle emission. The temperature and the plastic deformation effects are integrated into the deformation energy that will subsequently be used in modeling.

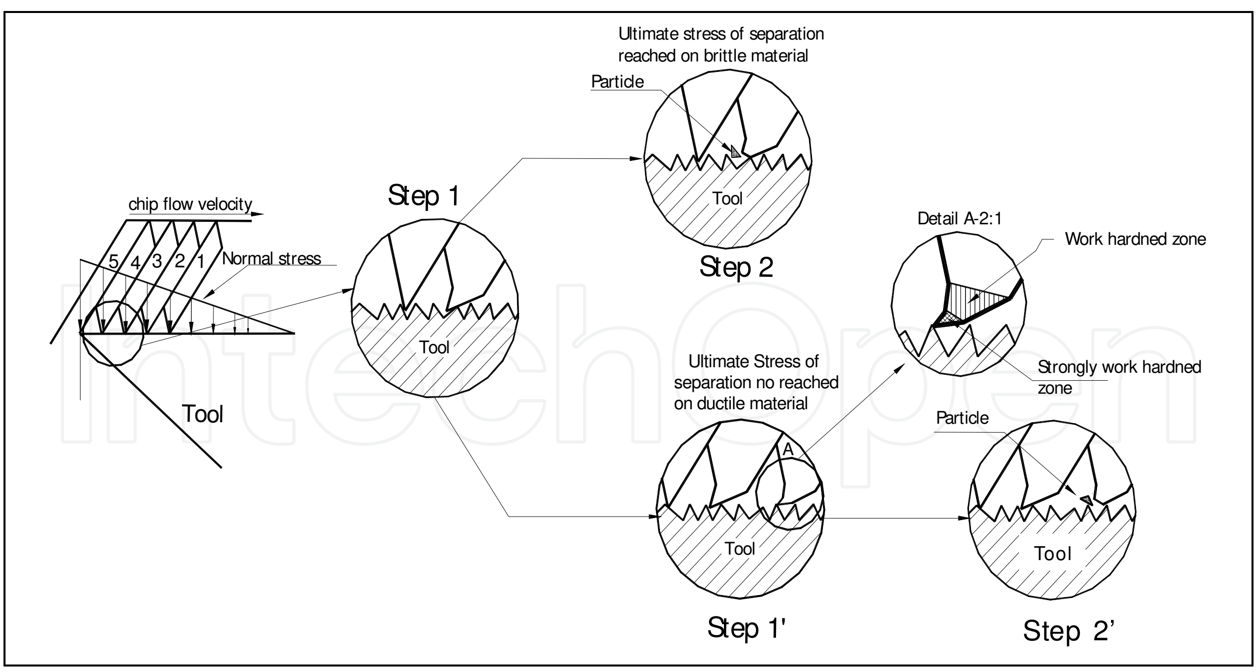

Fig. 13. Schematic illustration of mechanisms of dust emission at the chip-tool

The measurement system generates different types of information concerning the sampled dust, including the aerodynamic diameter, the stocks size, the electrical mobility etc. However, some transformations should be done to evaluate the mass, the volume or the number of particles when the concentration and the flow rate are known. It presents the dust particle concentration versus the acquisition time. Khettabi et al. (2007) propose a new more representative dimensionless index, which has a physical meaning, and allows a large-scale comparison. This new index is the ratio of the dust mass to the mass of chip removed from the workpiece material:

$$Du = \frac{m_{Dust}}{m_{Chip}} \tag{6}$$

where m_{Dust} (g) is the mass of total dust generated and m_{Chip} (g) is the mass of the chip produced.
The mass of the chip m_{chip} (g) is evaluated by multiplying the volume of material removed by the density.
Khettabi et al. (2010a) developed a hybrid model of particle emission during machining processes which was based on the energy approach, combined with macroscopic friction (tool-chip), microfriction, and plastic deformation of materials:

$$D_u = A \times \frac{\beta_{max} - \beta}{\beta_c} \times R_a \times \eta_S \cdot \left(\frac{V_0}{V}\right)^{\delta} \exp\left(\frac{-E_A}{\tan\phi(1 - C_h \sin\alpha)V_c \frac{F_{sh}}{bf}}\right) \tag{7}$$

where A is the factor of proportionality and δ is a material parameter introduced to characterize the capacity of the material to produce metallic dust. For each material, a constant δ is attributed. The parameter δ is experimentally determined to obey the following criteria (Eq. 8).

$$\delta \equiv \begin{cases} \delta \geq 1 \rightarrow Ductile \quad materials. \\ 0.5 < \delta < 1 \rightarrow semi-ductile \quad materials \\ 0 < \delta \leq 0.5 \rightarrow Brittle \quad materials \end{cases} \tag{8}$$

Aluminum alloys are generally considered to be ductile materials. For cast aluminum alloys: $0.5 \leq \delta \leq 1.0$ and for wrought aluminum alloys: $1.5 \leq \delta$ (6061-T6:δ=1.5)
All parameters in equation 7, such as the rake angle α, the shear angle ϕ, the cutting speed V, the feed f, the roughness Ra, βmax, and βc, can be known or easily determined. The shearing force and temperature can be measured directly or estimated, although measurements will be difficult in the case of some processes. Estimation is possible using the Needelman-Lemonds constitutive equations.
The predictive dust emission model (Eq. 7) is found to be in agreement with experimental results (Figs. 14, 15, 19, 20). An algorithm was programmed and used to simulate dust emissions during the dry machining of aluminum and steel alloy. Carbide tools with different geometries were used for different tests.
Brittle materials, such as cast aluminum alloy or gray cast iron, present a special behavior (Fig 15). In this case, zone III has disappeared, and dust emission is continuously increased

with the cutting speed. The decrease in dust emission at high speed (Fig.14, zone III) is attributed to the softening effect of the ductile materials, which is not the case for brittle materials such as cast aluminum alloy or gray cast iron (Fig. 15).

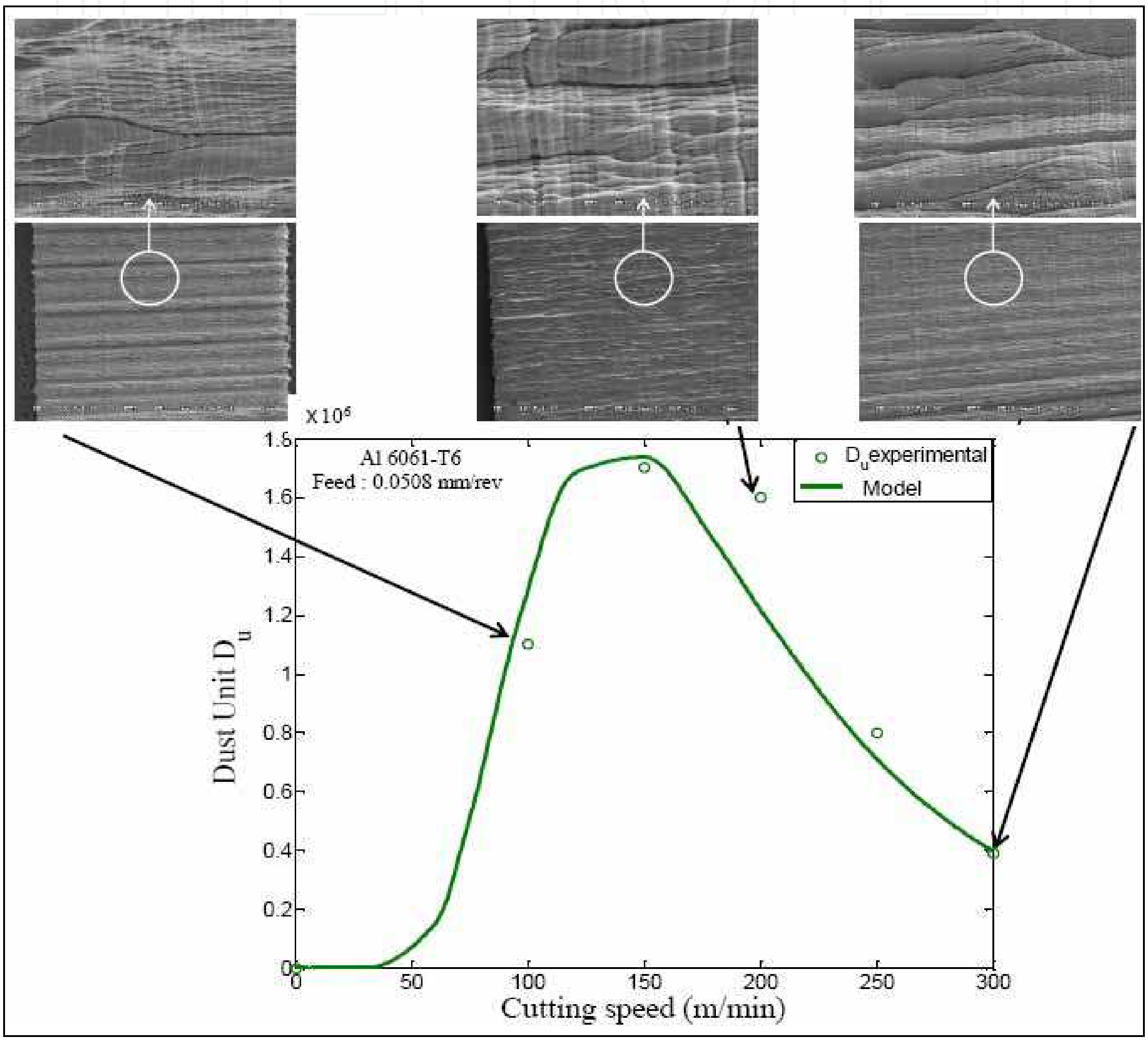

Fig. 14. Simulation results and experimental results for dust emission when dry machining Al 6061-T6

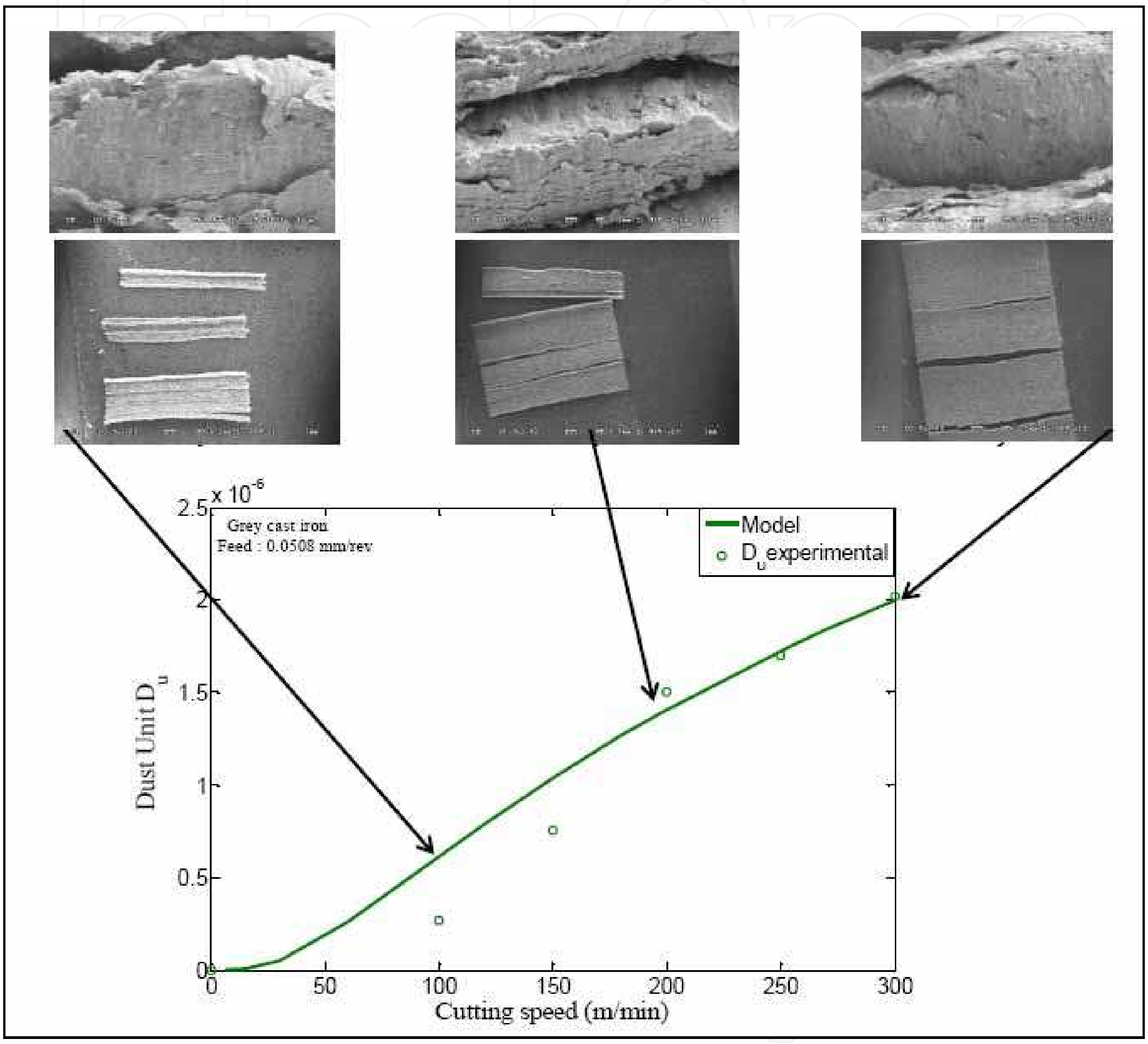

Fig. 15. Simulation results and experimental results for dust emission when dry machining gray cast iron

In the intermediate cutting speed range (zone II, between 100 and 150 m/min, Fig. 14), the particles emission is higher compared to the other ranges. The highest value of the particles emission corresponds to the critical value of the cutting speed that should be avoided. The critical cutting speed appears to be widely influenced by the workpiece material, and not by the machining processes (Khettabi et al., 2010b). It seems that the critical cutting speed depends significantly only on the workpiece material, and not on the machining processes, the tool geometry or the heat treatment. For the 6061-T6 aluminum alloy, the critical cutting speed is around 150 m/min during drilling, milling and turning (Figs. 16-18). It also observed that the critical cutting speed is still invariable for different rake angles and different lead angles.

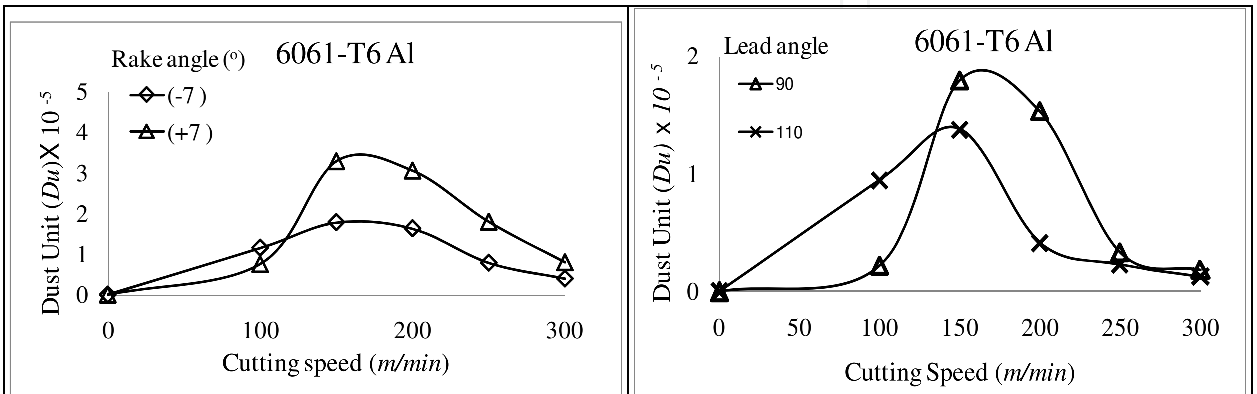

a) Orthogonal cutting | b) Oblique cutting

Fig. 16. Particle emission as a function of cutting speed and tool geometry during oblique and orthogonal cutting of 6061-T6 aluminum alloy

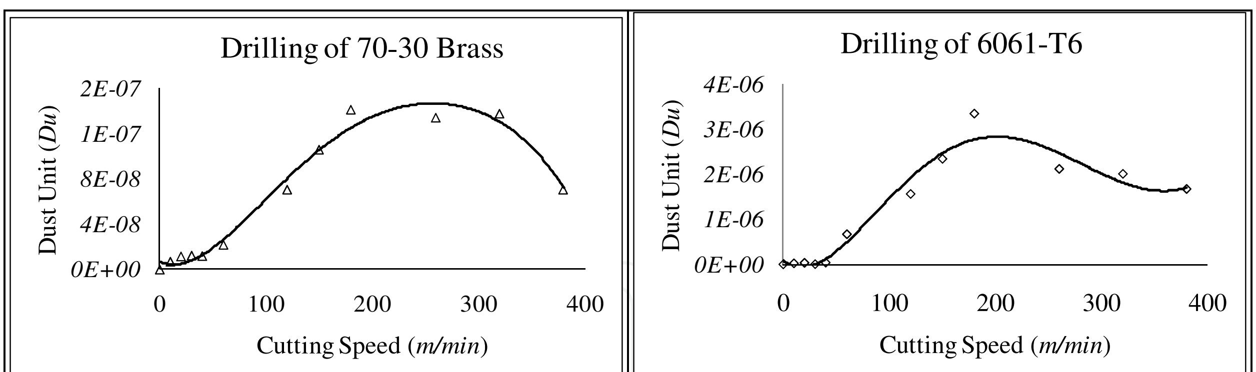

a) 70-30 Brass | b) 6061-T6 Aluminum alloy

Fig. 17. Particle emission during drilling of a) 6061-T6 aluminum alloy, and b) 70-30 Brass

Heat treatment influences the mechanical properties, and consequently, the quantity of particles emitted (Fig. 18). It was found that the critical value of the cutting speed, at which particle emission is at a maximum, depends on the material, and not significantly on the heat treatment. However the quantity of particles emitted at that critical speed depends on workpiece materials conditions (Fig. 18).
Figure 19 presents the simulation results (Eq. 7) for dust emission as a function of the feed and cutting speeds for dry machining of aluminum alloy 6061-T6. It was found that the

generated dust decreases with chip thickness, a result which is consistent with the experimental findings of Akarca et al. (2005) and Fang (2007). Therefore, an increase in the feed rate could reduce the amount of dust generated during machining. When the feed rate and cutting speeds both increase, the chip becomes more segmented, and consequently, the dust emission decreases.

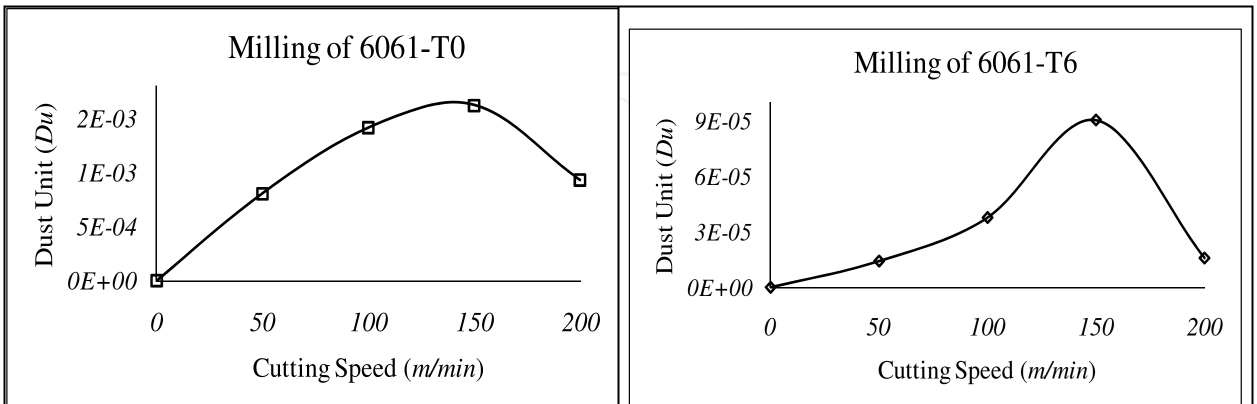

a) 6061-T0 Aluminum alloy | b) 6061-T6 Aluminum alloy

Fig. 18. Experimental (Du) during milling of aluminum alloy 6061-T6 and T0

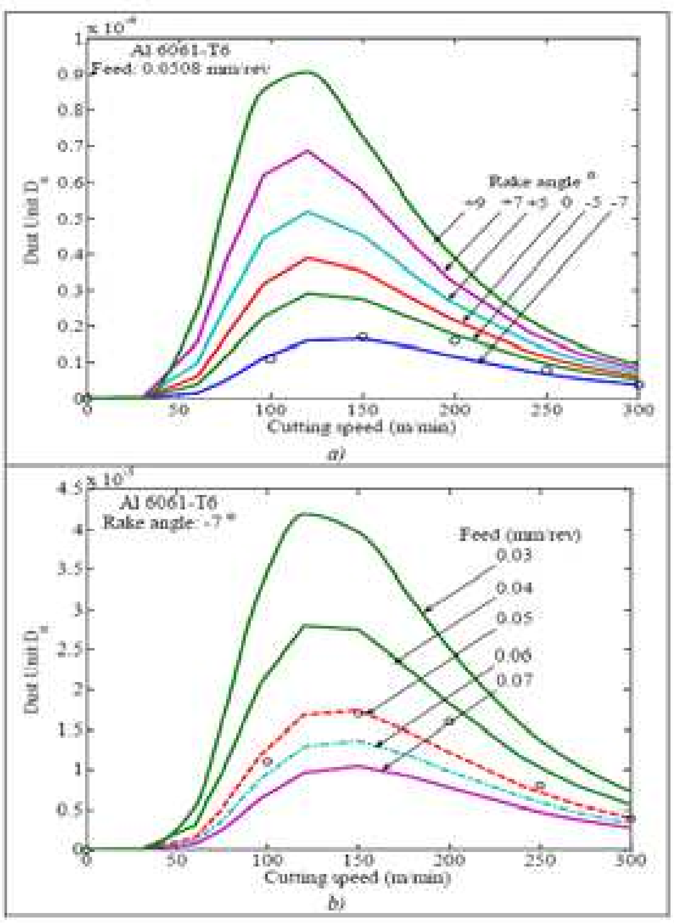

Fig. 19. Simulation results for particles emission during dry machining of Al 6061-T6 varying with cutting speed and: a) rake angle and b) feed

Figure 20 presents the simulation results (Eq. 7) for dust emission as a function of the tool rake angles and the cutting speeds for aluminum alloys, steels and cast iron. These results show good agreement with experimental data and the proposed model results (Figure 20). Even nanoparticle emission results during machining confirm the rake angle effect (Tönshoff et al, 1997). When the tool rake angle increases, the dust emission also increases.

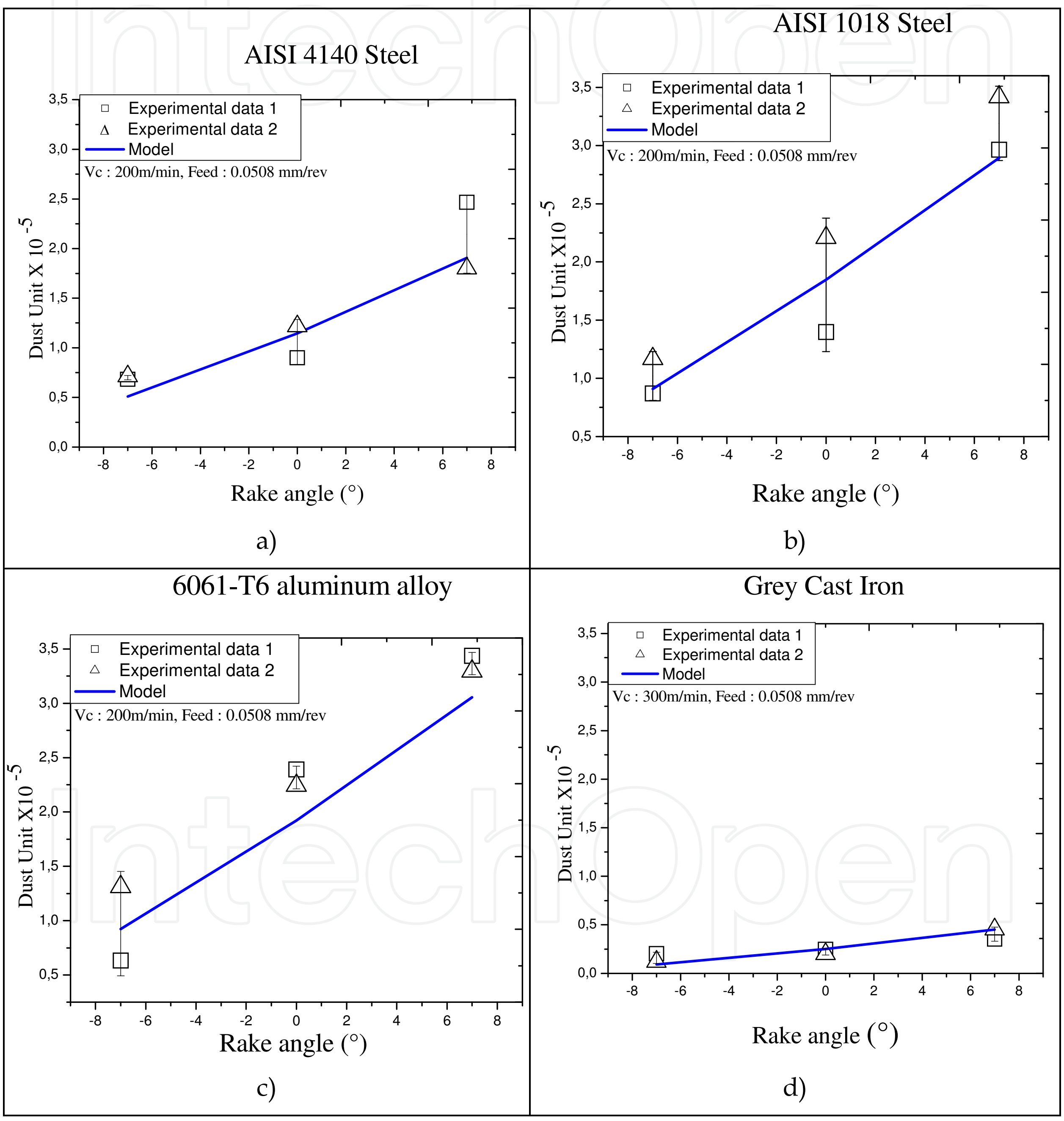

Fig. 20. Predicted dust emission data as given by equation 7 (line) compared to two experimental data of AISI 1018, AISI 4140 steels, gray cast iron and 6061-T6 aluminum alloy

3.4 Metallic particle size distribution

Size distribution as a function of the different concentrations shows a decrease in particles emission when cutting speed is increased (Figs. 21-22). A comparison for different aluminum alloys illustrate that particles emissions can decrease when the material toughness decreases (Figs. 21-22). Small-sized metallic particles, such as ultrafine particles, are known to be potentially more dangerous.

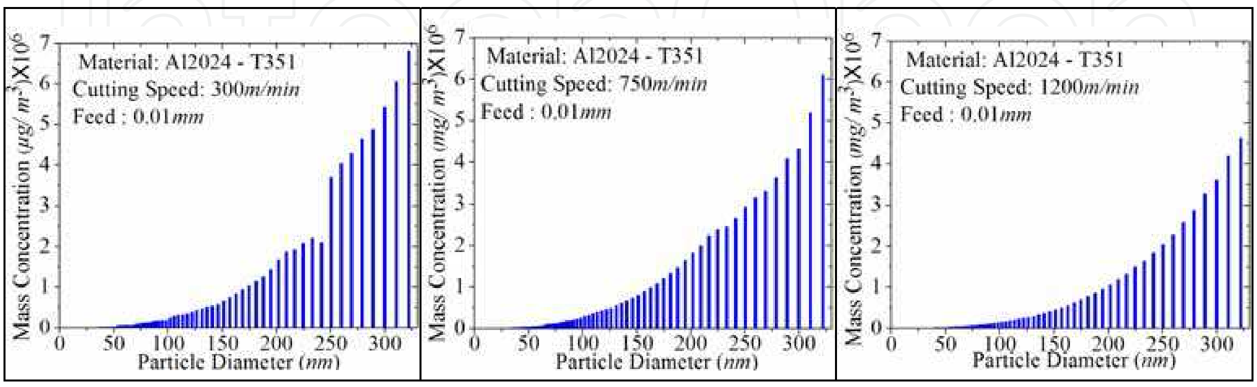

Fig. 21. Mass concentration as a function of size distribution for the 2024-T351 aluminum alloy

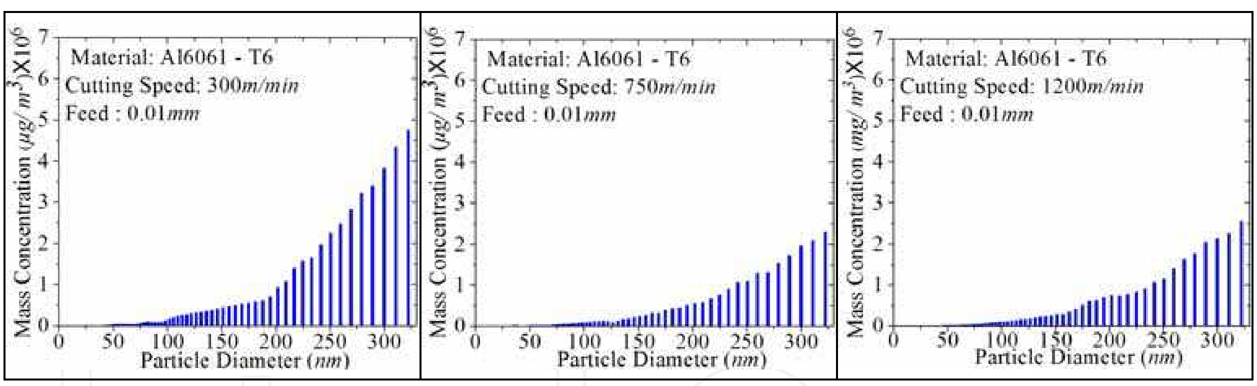

Fig. 22. Mass concentration as a function of size distribution for the 6061-T6 aluminum alloy

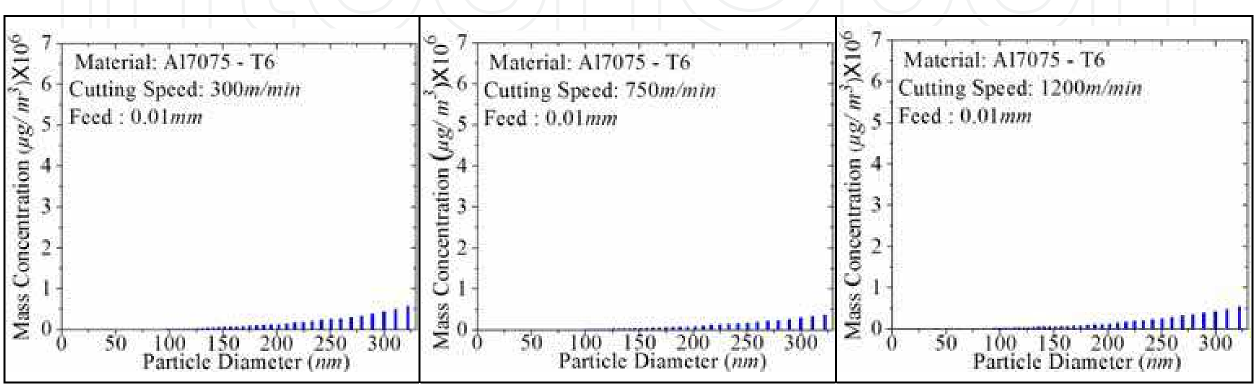

Fig. 23. Mass concentration as a function of size distribution for the 7075-T6 aluminum alloy

The combined influence of the cutting speed and the feed on the particle size depends on the workpiece material. During the milling process, the experiment shows that there is no homogenous influence of the cutting speed and the feed on the particle size for the materials tested (Fig. 23).
For purpose of analysis, it is very difficult to consider all particle size distributions, and for that reason, the mean size is considered as the particle size parameter. The mean particle size can be obtained by the following equation (Eq. 9):

$$Dm = \frac{\sum_{l}^{u} nD_P}{N} \tag{9}$$

where (N) is the total number of particles; (n) is the number (weighted) of particles per channel; (Dp) is the particle diameter (channel midpoint); (l) is the lower channel boundary, and (u) is the upper channel boundary.
For aluminum alloy 2024-T351, increasing the feed rate or cutting the speed enhances the mean particle size (Dm) until a certain value is reached, and then stagnation is observed (Fig. 24). The relatively low value of the mean particle size (Dm) was (23.4 nm) obtained for low feeds and speeds (0.01 mm/rev and 300 m/min).
For aluminum alloy 6061-T6, the influence of the cutting speed on the mean particle size (Dm) remains quite similar to what is seen in alloy 2024-T351, except that the influence of the feed rate for 6061-T6 is at a maximum at the intermediate value of feed. For low cutting speeds and low feed rates, it can be seen that there is a tendency for the mean particle size (Dm) to decrease (Fig. 24). Generally, it can further be seen as well that an increase in the feed rate can contribute to a decrease in the mean particle size (Dm) (Fig. 24). For aluminum alloy 7075-T6, the influence seems to be similar to the behavior of the aluminum alloys 2024-T351, with some variations. When both the cutting speed and the feed rate decrease, the value of the mean particle size (Dm) decreases (Fig. 24). The influences of the cutting speed and of the feed rate on the mean particle size (Dm) seem to trend in the same direction, but the variation in Dm is not very wide, especially for the aluminum alloys 6061-T6 and 7075-T6. For 6061-T6, the value of Dm is located between 131 nm and 173 nm nominal size, except for the smallest value, of about 50.2 nm. However, for the 7075-T6, the value of Dm is located between 125 nm and 146 nm.

4. Conclusion

The development of aluminum alloys is often conditioned by aeronautical requirements, but aluminum is very interesting for several applications in other sectors. Depending on the nuances, the composition, the treatments and the cutting conditions of these alloys, the material can be classified according to its machinability, recyclability, energy consumption and particle emission.
The machining of aluminum alloys is relatively easy as the cutting forces involved are low and the tool life is relatively high if there is no built-up edge or material adhesion problem. However, some problems may arise with the chip form and particle emissions. It is shown that long, continuous and spiral chips can indeed be prevented by selecting appropriate machining feeds and speeds.

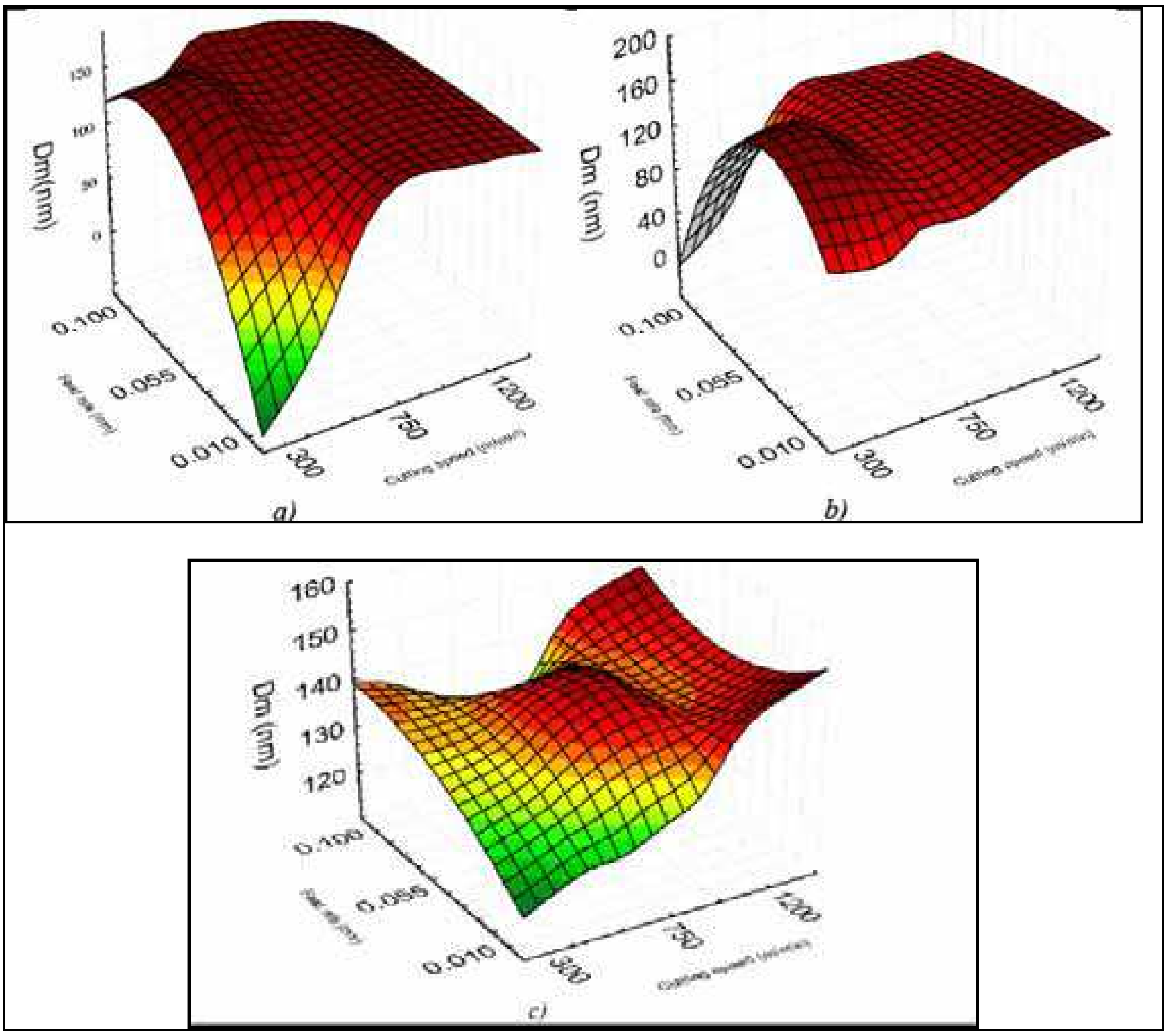

Fig. 24. Influence of the cutting speed and the feed rate on the mean particle size of the aluminum alloy: a) 2024-T351, b) 6061-T6, and c) 7075-T6

The machining of aluminum alloys generates fine and ultrafine particles, which have a relatively high sedimentation time and remain airborne for a long time, and could jeopardize the health of the worker. The machining of aluminum alloys using a special tool material and geometry during dry cutting at high speeds can be advantageous and sustainable.

5. References

Akarca, S.S. Altenhof, W.J. & Alpas, A.T. (2005). Characterization and Modeling of Subsurface Damage in a 356 Aluminum Alloy Subjected to Multiple Asperity Sliding Contacts, Minerals, *Metals and Materials Society*, Warrendale, PA, USA, 2005, p 107–120

Armarego, E. J. A. (1984). Predictive Models for Drilling Thrust and Torque- a comparison of three Flank Configurations. *Annals of the CIRP*, Vol. 33, No. 1, pp. 5-10.

Arumugam, P. U., Malshe, A. P., and Batzer, S. A., Bhat, D. G., 2002. Study of airborne dust emission and process performance during dry machining of aluminum-silicon alloy with PCD and CVD diamond coated tools NAMRC, *ID. Society of Manufacturing Engineers. MR02-153*, pp 1-8, May 21-24 2002 West Lafayette.

ASM Handbook, *Volume 16 – Machining*, Ninth edition, Joseph R. Davis senior Editor, page numbers (761-766), ISBN 978-0-87170-022-3, Metal Park, OH 44073

Balout, B., Songmene, V., Masounave, J. (2002). Usinabilité des alliages de magnésium et d'aluminium Partie I: Forces de coupe. proc. of the international symposium on enabling technologies for light metal and composite materials and their end-products, *41th conf. of metallurgists of CIM*, 2002 Vancouver, BC, Canada , pp. 223-242.

Balout, B, Songmene, V., Masounave, J. (2007). An experimental study of dust generation during dry drilling of pre-cooled and pre-heated workpiece material. *Journal of Manufacturing Processes*. Vol. 9, No. 1, pp. 23-34.

Becze and Elbestawi (2002). A chip formation based analytic force model for oblique cutting. *Int. Journal of Machine Tools and Manufacture*, Vol. 42. No. 4, pp. 529-538.

Demir H, Gündüz S. (2008). The effects of aging on machinability of 6061 aluminium alloy, *Journal of Material and Design*, doi:10.1016/j.matdes.2008.08.007

Fang, H.-W. (2007). Characteristic Modeling of the Wear Particle Formation Process from a Tribological Testing of Polyethylene with Controlled Surface Asperities, *J Appl. Polym. Sci.*,Vol. 103, pp 587–594.

Konig, W, Erinski D., 1983, Machining and Machinability of Aluminium Cast Alloys, *Annals of the CIRP*, Vol 32, N 2

Khettabi, R., Songmene, V and Masounave, J., (2007), Effect of tool lead angle and chip formation mode on dust emission in dry cutting, *Materials Processing Technology* 194 (1-3), pp.100-109.

Khettabi R., Songmene V., Zaghbani I. and Masounave J (2010a), Modeling of fine and ultrafine particle emission during orthogonal cutting, *Journal of Materials Engineering and Performance*, JMEPEG 19, pp. 776–789.

Khettabi, R., Songmene, V. and Masounave J. (2010 b). Influence of machining processes on particles emission, *49th Annual Conference of Metallurgists of CIM*, 4-6 Oct. 2010, Vancouver, BC, Canada, pp. 277-288.

Kouam J., Masounave J. and Songmene V. (2010). Pre-holes Effect on Cutting Forces and Particle Emission During Dry Drilling, *49th Annual Conference of Metallurgists of CIM*, 4-6 Oct. 2010, Vancouver, BC, Canada, pp. 253-263.

Mackerer, C. R., (1989). Health Effects of Oil Mists: A Brief Review, *Toxicology & Industrial Health*, Vol. 5, pp. 429-440.

Ostiguy C, Roberge B, Ménard L, Endo C.A. (2008). Guide de bonnes pratiques favorisant la gestion des risques reliés aux nanoparticules de synthèse, *Guide technique R-586*, Études et recherches, IRSST, Montréal, Canada, 2008, pp. 73

Roy P. Sarangi S.K; Ghosh. A.; Chattopadhyay A.K., (2008), Machinability study of pure aluminium and Al–12% Si alloys against uncoated and coated carbide inserts, *Int. Journal of Refractory Metals & Hard Materials*. In press

Shaw, M.C. (2005). Metal Cutting Principles, 2nd edition, Oxford, New York, chap 9, pp. 183.

Songmene V., Masounave J., & Khettabi R. (2007). Safe, environmentally-friendly and cost effective machining. Safety, Health and Environmental World Congress, Santos, Brasil, July 22-25, 2007, pp. 44-48

Songmene V., Balout B., & Masounave J. (2008). Clean Machining: Experimental Investigation on Particle Formation, Part II: Influence of Machining Strategies and Drill Condition, *Int. J Environmental Conscious Design & Manufacturing, (ECDM)*, 2008, Vol. 14, No. 1, pp. 17–33

Subramanian, K., and Cook, N., H. (1977). Sensing of Drill Wear and Prediction of Drill Life. *J of Engineering for Industry*, Trans of ASME, Vol. 99, Serie B, pp. 295-301.

Tönshoff, B. Karpuschewski, & T. Glatzel, (1997). Particle Emission and Emission in Dry Grinding, *Annals of the CIRP*, Vol. 46, No. 2, pp. 693–695.

Xie, J.Q., Bayoumi, A.E. & Zbib, H.M. (1996). Study on shear banding in chip formation of orthogonal machining. *Int. J Machine Tools & Manufacture*, Vol. 36, No. 7, pp. 835-847.

Tash M., Samuel F.H., Mucciardi F., Doty H.W., Valtierra S., (2006), Effect of metallurgical parameters on the machinability of heat-treated 356 and 319 aluminum alloys, J. *Materials Science and Engineering*, Vol. 434, pp. 207–217

Zaghbani I. and Songmene V. (2009a) A force-temperature model including a constitutive law for Dry High Speed Milling of aluminium alloys, *Materials Processing Technology*, 2 0 9 (2 0 0 9) pp 2532–2544.

Zaghbani, I., Songmene, V. and Khettabi, R., (2009b), Fine and Ultra fine particle characterisation and Modeling In High Speed Milling of 6061-T6 Aluminium Alloy; *Journal of Materials Engineering and Performance*, Vol.18, Issue 1 (2009), pp 38-49.

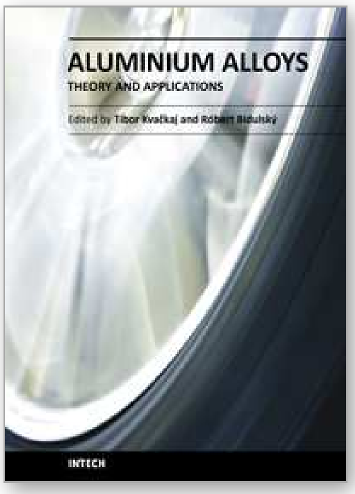

Aluminium Alloys, Theory and Applications
Edited by Prof. Tibor Kvackaj

ISBN 978-953-307-244-9
Hard cover, 400 pages
Publisher InTech
Published online 04, February, 2011
Published in print edition February, 2011

IntechOpen